Time evolution of the Earth's geomagnetic pole based on Portuguese paleomagnetic samples

Demur Merkviladze, Jakub Morawski & Maria Utkina

January 15, 2024

Abstract

The report summarizes a project investigating various ways in which geomagnetic pole position time series can be visualized. A review of basic paleomagnetical concepts and the theory behind the Virtual Paleomagnetic Pole is provided. Different ways of plotting the Virtual Geomagnetic Pole (VGP) location time series (simple, polar, with B-spline interpolation) are discussed, highlighting their advantages and disadvantages. Other visualisation concepts are developed as well: animation and a widget application with a graphical user interface. A test case study is performed with input data based on a site in Portugal, provided by the paleomagnetic laboratory of the University of Coimbra. The results reveal known phenomena in the Earth's magnetic history, most notably the Laschamp excursion around 40000 years ago.

1 Introduction

In this project we developed a program to visualize time evolution of a geomagnetic pole. A geomagnetic pole is a point on Earth (characterized by geographic coordinates $\lambda_{\mathrm{GP}}, \varphi_{\mathrm{GP}}$) corresponding to a magnetic dipole which is a first order approximation of the Earth's magnetic field. The Earth's magnetic field, as explained in Butler 1992, can be characterized as follows:

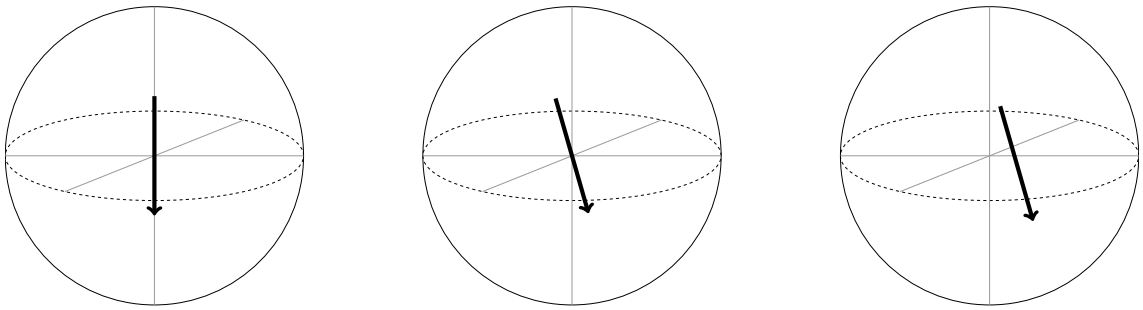

Figure 1: Schematic representation of the three dipole models described below. **Left**: geocentric axial dipole. Fixed orientation and center, magnitute can vary. **Center**: inclined geocentric dipole - same but arbitrary orientation. **Right**: eccentric dipole, where the center of the dipole is no longer fixed in the Earth's center.

- In the most basic model, one can imagine a dipole aligned with the center of the planet and parallel to the rotation axis. This simple *geocentric axial dipole model* can be convenient for deriving some of the associated equations but fails to accurately reproduce data obtained from paleomagnetic samples.
- Relaxing the assumption about the direction of the dipole vector, we come to the ***inclined geocentric dipole*** - a dipole of arbitrary (time-dependent) magnitude M and orientation, the latter corresponding to the aforementioned ***geomagnetic pole***. The inclined geocentric dipole (with the optimal fit of parameters) is capable of accounting for 90% of the Earth's magnetic field. The advantage of this approximate model is that it provides an accurate but simple way to illustrate the main features of the field and to study it's evolution over time.
- A more precise match between the data from measurements and the model can be achieved by relaxing the assumption about the central alignment. The *eccentric dipole* model continues to assume that the Earth's

magnetic field is produced by a magnetic dipole, but on top of allowing a variation of the magnitude and direction, the center of the dipole may be shifted from the Earth's center as well. The contemporary best-fitting eccentric dipole is shifted from the planet's center by about 500 km, or $\sim 8\%$ of the planet's radius. While it matches exactly the magnetic field measured at some locations on the globe, in some others there is still a discrepancy of up to 20%.

- The residual field, which cannot be explained by the best-fitting eccentric dipole, is referred to as Earth's *nondipole field* (see Fig. 2). It can be characterized (roughly) as a sum of several continental-scale features, which are modelled as smaller dipoles placed closer to the surface of the planet (mathematically anyways, the physical interpretation of those dipoles is not robustly established).

From this overview about the Earth's magnetic field it is rather clear that it would not be possible to infer a viable model of this field (on the global scale) based on a paleomagnetic measurement conducted in one site only. Even the simplest of the accurate models, the inclined geocentric dipole, may have a different corresponding geomagnetic pole depending on the site where the measurements were done and how strong was the nondipole field at that location. Therefore, the inclined geomagnetic dipole and the geomagnetic pole are generally modelled by averaging measure-

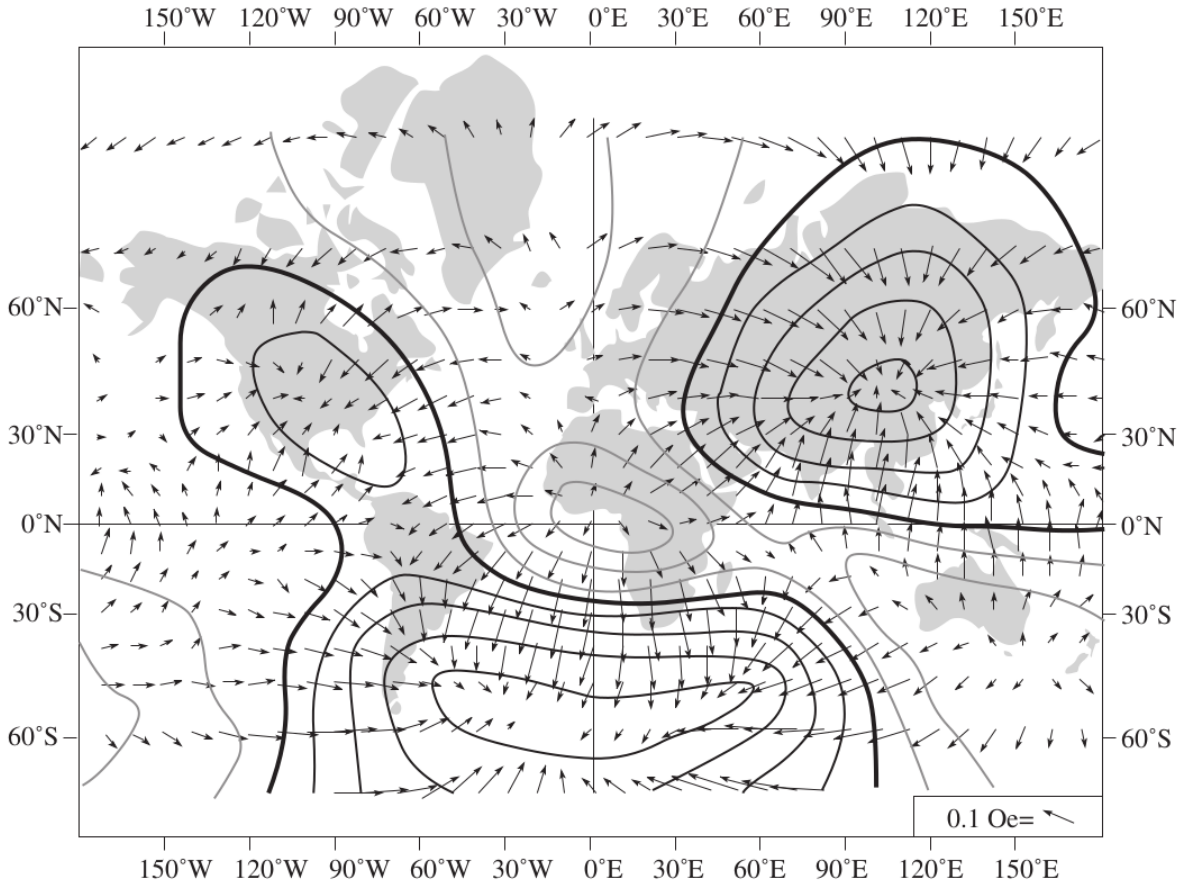

Figure 2: The nondipole geomagnetic field in the year 1945, figure from Butler 1992. Arrows indicate the magnitude and direction of the horizontal component on the nondipole field. Contours indicate lines of equal vertical component intensity: heavy black for 0, thin black for positive and grey for negative vertical component. The contour interval is 0.02 Oe

ments made at different locations. That's where the term ***virtual geomagnetic pole*** (VGP) comes in - a pole inferred based on data from a single location.

For our project, we were given a data set describing an evolution of the magnetic field vector $\mathbf{H}$ with time (the period between $\sim 50 - 30$ thousands of years ago) in a single location in Portugal ($\lambda_{\text{site}} = 39°32.891'N$,$\varphi_{\text{site}} =° 46.266'W$). The data were gathered and made available to us by the paleomagnetic laboratory of the University of Coimbra. It comes from preprocessed measurements evaluated with the *LSMOD.2* model of Korte *et al.* 2019.

We created a Python program which calculated the coordinates $\lambda_{\mathrm{VGP}}, \varphi_{\mathrm{VGP}}$ of the virtual geomagnetic pole based on such a data set and visualizes the time evolution of the VGP, both with static plots and animations. In the section 2, we review the mathematical theory behind the equations which were used in our code to calculate VGP locations. In section 3, we describe the process of determining the VGP and various functionalities offered by our code, as exemplified by the evaluation of our data set. In 4, we evaluate the evolution of the site's VGP in the light of generally established scientific knowledge about the Earth's paleomagnetic history. In 5, we elaborate on how our code could be developed to provide a more robust framework for computing and visualizing the temporal evolution of the virtual and actual geomagnetic poles.

2 VGP Calculation

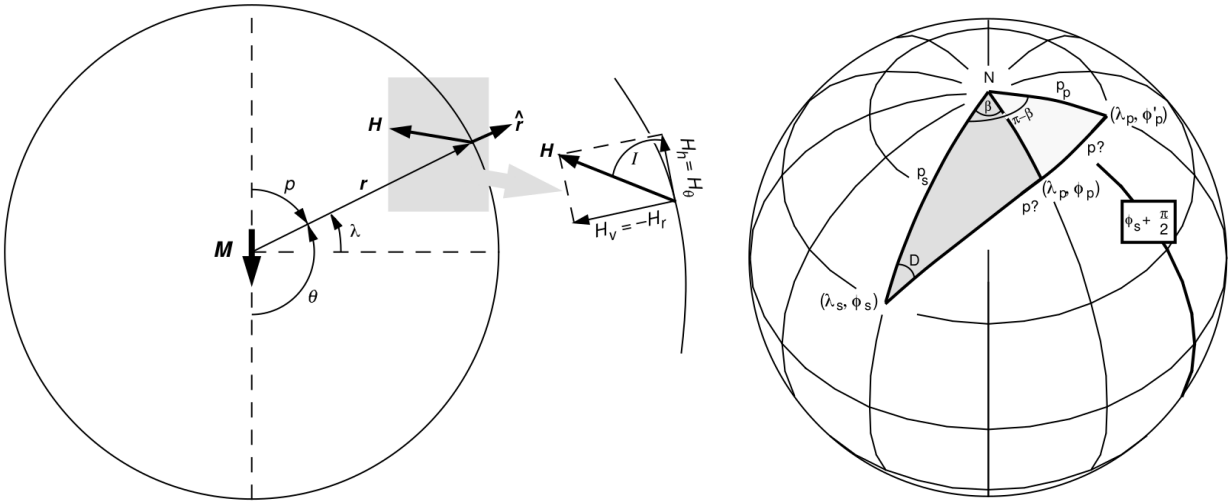

Figure 3: Figures from Butler 1992, illustrating the angles describing the orientation of the magnetic field vector and the derivation of the formulas for VGP coordinates. **Left**: Definition of the inclination angle. **Right**: declination and possible VGP locations. Symbols are explained in the text of section 2.

2.1 Dipole equation

Before we show how the formulas for VGP coordinates are derived, we need to derive the formula known as the **dipole equation**. For this, we will be considering the simplest of the models delineated in 1, the geocentric axial dipole. The equation correlates the angle I with the angular distance p from the geomagnetic pole. The **inclination** is, by definition, an angle between the magnetic field vector and it's component tangent to the globe, as shown on the left of Figure 3. For a geocentric axial dipole, $p = 90° - \lambda$, where λ is a latitude of a site. To correlate these two angles, one has to start from the scalar magnetic potential of a magnetic dipole, which is:

$$V = \frac{M \cos\theta}{r^2}$$

where $\theta = 90° + \lambda$ is an angle between the dipole and the site's position vector, as shown on the left of Figure 3. The magnetic field is then derived by differentiating the potential:

$$\mathbf{H} = -\nabla V = -\frac{\partial}{\partial r}\left(\frac{M\cos\theta}{r^2}\right)\hat{\mathbf{e}}_r - \frac{1}{r}\frac{\partial}{\partial\theta}\left(\frac{M\cos\theta}{r^2}\right)\hat{\mathbf{e}}_\theta = \frac{2M\cos\theta}{r^3}\hat{\mathbf{e}}_r + \frac{M\sin\theta}{r^3}\hat{\mathbf{e}}_\theta$$

On the other hand, $\mathbf{H} = H_r\hat{\mathbf{e}}_r + H_\theta\hat{\mathbf{e}}_\theta$, and by definition (see Figure 3):

$$\tan I = \frac{-H_r}{H_\theta} = -\frac{\frac{2M\cos\theta}{r^3}}{\frac{M\sin\theta}{r^3}} = -\frac{2}{\tan\theta} = -\frac{2}{\tan(90° + \lambda)} = 2\tan\lambda$$

The final result of $\tan I = 2\tan\lambda$ is known as the dipole equation, although it is useful to also keep in mind the equivalent version of $\tan I = \frac{2}{\tan p}$, as we will see in 2.2.

2.2 VGP

Now we can move to the case of the inclined geocentric dipole and consider a situation shown on the right of the Figure 3. The two sites marked as $(\lambda_p, \Phi_p), (\lambda_p, \Phi'_p)$ on the figure (here we will use a different notation though, namely $\lambda_{\text{VGP}}, \varphi_{\text{VGP}}$) are two potential locations of the geomagnetic pole (see two cases of the formula at the end of this section). The tangent component of the vector $\mathbf{H}$, i. e. $H_\theta \hat{\mathbf{e}}_\theta$ from the derivation in 2.1, would still be pointing toward that pole. Now that the geomagnetic pole no longer coincides with the North Pole as defined by the Earth's rotation axis, an angle of **declination** can be introduced as the angle between the magnetic field vector and the direction to the North Pole (interpreted as an angle between two planes passing through the center of the globe, as is the standard in spherical trigonometry). To find λ_{VGP}, the law of cosines of the spherical trigonometry can be used:

$$\cos(90^\circ - \lambda_{\text{VGP}}) = \cos(90^\circ - \lambda_{\text{site}}) \cos p + \sin(90^\circ - \lambda_{\text{site}}) \sin p \cos D$$

where p is the angle between the geomagnetic pole (VGP) and the site, with a corresponding arc on the surface of the sphere being one of the two arcs makred as p? on the figure. Simplifying this leads to:

$$\sin \lambda_{\text{VGP}} = \sin \lambda_{\text{site}} \cos p + \cos \lambda_{\text{site}} \sin p \cos D \iff \lambda_{\text{VGP}} = \arcsin(\sin \lambda_{\text{site}} \cos p + \cos \lambda_{\text{site}} \sin p \cos D)$$

and the angle p can be calculated from the inclination using the dipole equation from 2.1: $p = \arctan\left(\frac{2}{\tan I}\right)$.

Now, if $\Delta\varphi = \varphi_{\text{VGP}} - \varphi_{\text{site}}$, then from the law of sines of the spherical trigonometry we have:

$$\frac{\sin(90^\circ - \lambda_{\text{VGP}})}{\sin D} = \frac{\sin p}{\sin \Delta\varphi} \implies \Delta\varphi = \beta \vee 180^\circ - \beta$$

where

$$\beta = \arcsin\left(\frac{\sin p \sin D}{\cos \lambda_{\text{VGP}}}\right)$$

This ambiguity between two possible values of $\Delta\varphi$ is also shown on the right of the Figure 3. It can be resolved by using the spherical law of cosines again, this time to express $\cos p$ as:

$$\cos p = \cos(90^\circ - \lambda_{\text{VGP}}) \cos(90^\circ - \lambda_{\text{site}}) + \sin(90^\circ - \lambda_{\text{VGP}}) \sin(90^\circ - \lambda_{\text{site}}) \cos \Delta\varphi \iff$$

$$\iff \cos \lambda_{\text{VGP}} \cos \lambda_{\text{site}} \cos \Delta\varphi = \cos p - \sin \lambda_{\text{VGP}} \sin \lambda_{\text{site}}$$

Since $\lambda_{\text{VGP}}, \lambda_{\text{site}} \in [-90^\circ, 90^\circ]$, the cosine of both of those angles is nonnegative, and we can conclude that the sign of $\cos \Delta\varphi$ is determined by the sign of the right hand side $(\cos p - \sin \lambda_{\text{VGP}} \sin \lambda_{\text{site}})$. This helps us resolve the ambiguity, leading to the final formula of :

$$\varphi_{\text{VGP}} = \begin{cases} \varphi_{\text{site}} + \arcsin\left(\frac{\sin p \sin D}{\cos \lambda_{\text{VGP}}}\right) & \text{if } \cos p \geqslant \sin \lambda_{\text{site}} \sin \lambda_{\text{VGP}} \\ \varphi_{\text{site}} + \pi - \arcsin\left(\frac{\sin p \sin D}{\cos \lambda_{\text{VGP}}}\right) & \text{if } \cos p < \sin \lambda_{\text{site}} \sin \lambda_{\text{VGP}} \end{cases}$$

3 Virtual Geomagnetic Pole visualization

3.1 Data processing

The data we received from the paleomagnetic lab is a single file *LSMOD2_predictions.dat* with the following columns (as defined in the file header):

- Age (ka BP) - corresponding age of a sample in thousands of years
- D(deg.) - declination of $\mathbf{H}$ in degrees (see section 2 for definition)
- I(deg.) - inclination of $\mathbf{H}$ in degrees (see section 2 for definition)
- F(microT) - magnitude of $\mathbf{H}$ in μT

Independently, we were provided with the coordinates of the site ($\lambda_{\text{site}} = 39^\circ 32.891' N$,$\varphi_{\text{site}} =^\circ 46.266' W$, as mentioned in 1).

To be able to process this data, as well as potentially any similar files corresponding to other sites or models, we created a class **site_data** to load data from the file, store it in *NumPy* arrays and precalculate other useful time

series related to the evolution of VGP, as elaborated in the following sections. To create an object of that class, a user must provide the coordinates of the site and the file path expressed as strings, plus information on how many lines of the file should be skipped as a header (1 in our case). A detailed description of the class and it's functionalities can be found in the markdown documentation provided in our Jupyter Notebook.

Creating an object of our class **site_data** automatically calculates the VGP coordinates based on the data file for each moment in time, based on equations derived in section 2.

3.2 Visualizing the VGP evolution with a static plot

The main focus of the programming work was an exploration of different ways to visualize the temporal evolution of the VGP location. Defined, for a given moment in time, by a pair of coordinates $\lambda_{\mathrm{VGP}}, \varphi_{\mathrm{VGP}}$, the virtual geomagnetic pole is a point on a sphere with which we approximate the shape of the globe. Most methods of data visualization, however, are intrinsically 2-dimensional. While a projection of a sphere on a plane (such as in Figures 1 and 3 right), with a relevant VGP point highlighted, could be a way to illustrate these changes, it would be a difficult format to interpret unless sophisticated 3D animation techniques were applied in a software such as Blender (which could be an interesting task to undertake, but would be beyond the scope and focus of this project). Therefore, we set our attention on different ways to visualize the VGP evolution on a 2-dimensional plot.

3.2.1 Simple and polar plots

A *simple* plot, such as Figure 4 left, on which the value of each coordinate $(\lambda_{\mathrm{VGP}}, \varphi_{\mathrm{VGP}})$ is plotted against time, is a basic way to visualize the paleomagnetic variability, frequently used in literature, including Korte *et al.* 2019. While it can serve as an easy way to differentiate between periods of low and high variation, and a closer look at the slopes of each curve on the plot could reveal the general direction in which the VGP was travelling at any given moment, the broader understanding of the nature and scope of these changes eludes human intuition from looking at a simple plot alone.

In order to better grasp the geometric nature of the phenomenon, and obtain a more intuitive visualization, we dove into ways of demonstrating the temporal evolution of the VGP on a *polar* plot. Figure 4 presents a comparison between the two types of plots, generated for a period with low variability, where the advantage of a polar plot is even more striking. The polar plot which we are using, operates in a space where the angle is equal to the longitude, and the radius is equal to $90° - \lambda$, so as to be centered on the North Pole. A color map is used to indicate the time coordinate, with both points and lines between points following a sequence of colors indicated by the color bar.

There is one conceptual challenge when interpreting a polar plot of such kind if the range of latitude variations is too large. While a small spherical cap can be well approximated by the circle, if the latitudes transcend the equator down to the southern hemisphere, as is the case during the Laschamp Excursion (see 4), this form of visualisation presents the globe in a very distorted way. In essence, the method of presenting VGP locations on such a polar plot is equivalent to the stereographic projection mapping, and the distortion of the points on the southern hemisphere is same as in that projection. (see Maths n.d.). In order to make the plots less confusing, if positions from the southern hemisphere need to be included, we indicate the equator with a thick line and mark the area corresponding to the southern hemisphere in gray, with labels **N** and **S** marking areas corresponding to each hemisphere (see Figures 5, 6,9,10).

Despite the name, the simple plot has it's own challenges. Specifically, the question of how to best represent the time series of the longitude angles does not have a universal answer. Suppose that at one point in time, $\varphi_{\mathrm{VGP}} = 350°$ and at the next one $\varphi_{\mathrm{VGP}} = 10°$. The most logical interpretation, in terms of the continuous behavior of a periodic variable, is that it went through an intermediate value of $360° \equiv 0°$. However, if we plotted the values as they are, we would see an illusion of a lack of continuity, where the φ_{VGP} would take "the long way round" through the range of values decreasing from 350° to 10°. To prevent that confusing apparent lack of continuity, we introduced a threshold on the proximity of the difference of two consecutive longitudes to 360°, and if it fit under the threshold, we would shift all longitudes after that point by 360° in the appropriate direction, so that the variable would be continuous on the plot. An example of the visually pleasing result obtained by setting a generous threshold of 100° for plots related to different subperiods can be found on Figure 9. However, when generating a plot for a longer period, if an analogous exception occurred multiple times in the same direction, the range of the ordinate on the plot would swell disproportionately, leading to illegibility of the latitude part. To avoid this, a correction is not made in the same way when plotting the entire period on Figure 10, but the sacrifice in terms of the intuitiveness of the longitude continuity

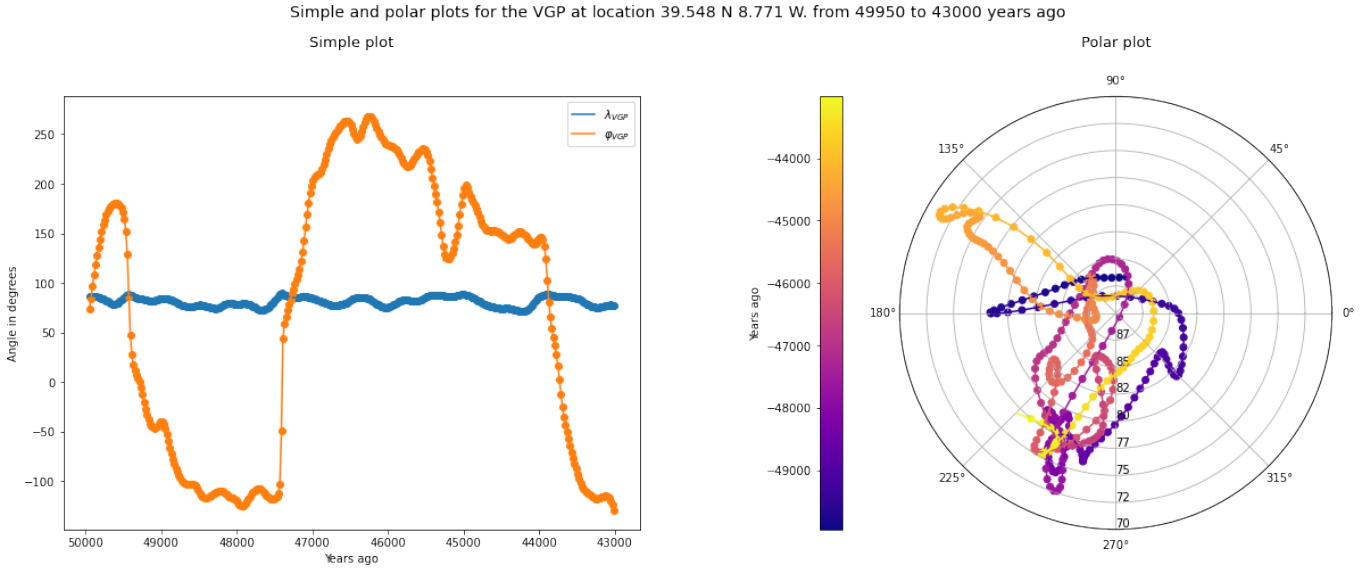

Figure 4: Two ways of visualizing the evolution of the VGP position over time, exemplified on the period without drastic changes of the Earth's magnetic field (see section 4). **Left**: Plotting the evolution of each coordinate (latitude λ_{VGP} and longitude φ_{VGP} independently. While a scrutiny of each curve could help delineate periods of eastward, westward, northward and southward drifts of the VGP location, it is difficult to gain a thorough understanding of these changes from looking at that plot alone. **Right**: Polar plot centered on the North Pole, with $90° - \lambda_{\text{VGP}}$ as the radial coordinate. The circular area of the plot can in most cases (except for the Laschamp Excursion where the VGP transcends to the southern hemisphere, see Figure 5) be interpreted as a spherical cap where the variation of the VGP position is taking place, projected onto a plane. This form of visualization is helpful to understand the general behavior of the VGP location and the directions it has travelled to with time.

perception is inevitable.

The visualization method which utilizes a polar plot inspired an idea of creating an animation (3.3) that would demonstrate the variation of the VGP position in a dynamic way. A demand for an aesthetic way to demonstrate these changes on an animation, in the face of the fact that in some periods the separation between two consecutive VGP locations may be large (see 5, 4), inspired the idea of utilizing B-spline interpolation in the polar plots, which we will elaborate on in the following section.

3.2.2 Cubic B-spline interpolation

On the right side of Figure 4, points corresponding to consecutive VGP locations are very close to each other, and connecting them with a straight line does not deteriorate the appearance of the plot. However, this is not always the case, in particular in the Earth's magnetic field history there were occurrences of drastic changes at short timescales, such as the Laschamp Excursion (see Section 4), for which two consecutive measurements (or outputs of a model) may differ a lot. As we can see on the left of Figure 5, linear interpolation between such strongly separated data points makes a polar plot less legible and less aesthetic. In particular, it would not be very suitable for animating in a way that we introduce in 3.3.

Inspired by techniques used in computer graphics, we used **B-spline interpolation** to counterbalance this issue and connect consecutive points with smooth curves, such as on the right side of the Figure 5. The term B-spline interpolation refers to an evaluation of a curve between given points, called *knots*, with a set of polynomial functions of a given degree evaluated at each interval between the knots. Specifically, using a *SciPy.interpolate* function ***splprep*** (Scipy-documentation n.d.) a construction of a B-spline interpolated curve of degree k in 2 dimensions goes as follows:

1. If a series of $m+1$ knots $p_0, p_1, ..., p_m$ is a series of points defined in cartesian coordinates as: $\forall_{i \in \{0,1,...,m\}} p_i =$

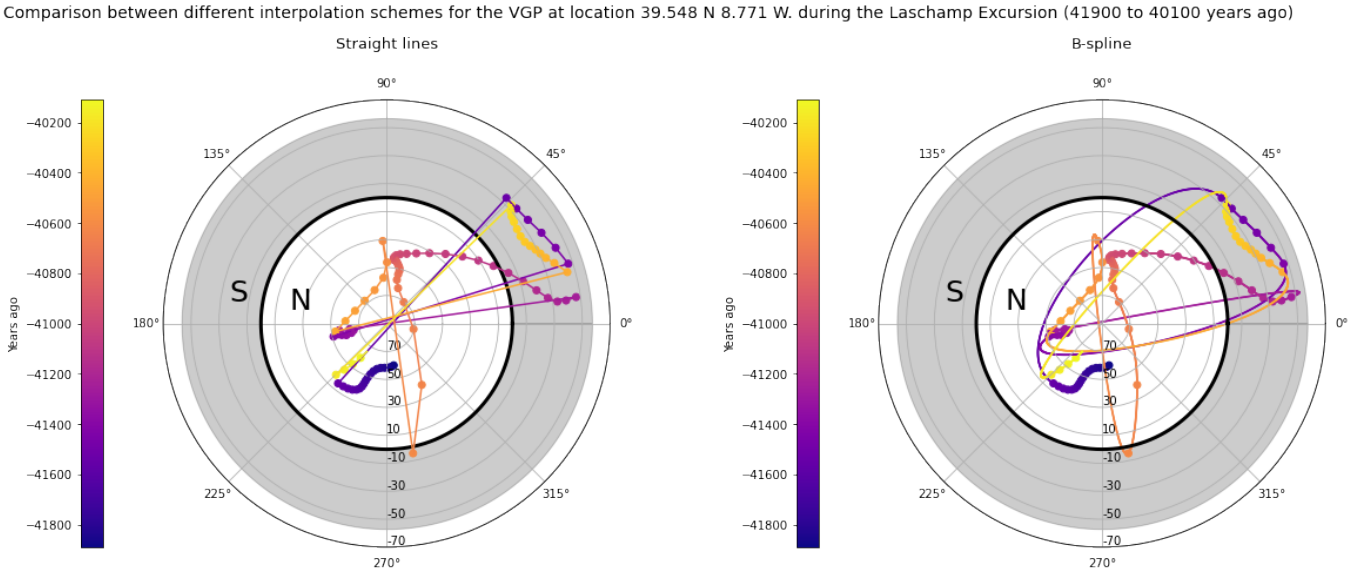

Figure 5: Two ways of visualizing the evolution of the VGP position on a polar plot, exemplified on the period with the most violent changes of the Earth's magnetic field (see section 4). Thick line marks the equator and parts of the plot corresponding to each hemisphere are indicated on the plot, see discussion in 3.2.1. **Left**: Positions calculated for each data point are connected with straight lines. The color of each line and point corresponds to the moment in time. The use of straight lines ensures no bias and the most faithful representation of the phenomenon. **Right**: same, but using B-spline interpolation to obtain a smooth curve. The result is much more easthetic, however, the features such as the big purple arc on the left have no supporting evidence in the data and may thus be misleading.

(x_i, y_i), each i^{th} knot is associated with a value u_{i+k} such that

$$u_k = 0 \wedge \forall_{i\in\{1,\dots,m\}} u_{i+k} = \frac{\sum_{j=1}^{i} d(p_j, p_{j-1})}{\sum_{k=1}^{m} d(p_k, p_{k-1})}$$

where $d((x,y),(u,v)) = \sqrt{(x-u)^2 + (y-v)^2}$ is the cartesian distance. We then complement these to a sequence of numbers $(u_0, u_1, ..., u_{m+k})$ by setting the remaining elements of the sequence to 0 or 1, such that

$$0 = u_0 = u_1 = ... = u_k < u_{k+1} ... < u_{m-1} < u_m = u_{m+1} = ... = u_{m+k} = 1$$

The equation above is an essential condition for a correct setup of B-spline knot arguments to interpolate a curve with B-splines of degree k. A different way of assigning u_i values, within the constraints of that equation, could be achieved by providing a vector input to the keyword u of the function ***splprep*** (Scipy-documentation n.d.), however, a notion that a situation where such a change would be beneficial could occur seems highly improbable.

2. A k^{th} degree B-spline functions of a variable $u \in [0,1]$ are generated in a recursive manner:

   (a) 0^{th} degree B-splines are given as constant functions equal to 1 at given intervals:

   $$\forall_{i\in\{0,1,\dots,m\}} B_{i,0}(u) = \begin{cases} 1 \text{ if } u_i \leqslant u \leqslant u_{i+1} \\ 0 \text{ otherwise} \end{cases}$$

   (b) For any $\kappa \in \mathbb{N}$, B-splines of degree $\kappa + 1$ are generated based on B-splines of degree p, based on a recursive formula:

   $$\forall_{i\in\{0,1,\dots,m\}} B_{i,\kappa+1}(u) = \frac{u - u_i}{u_{i+\kappa+1} - u_i} B_{i,\kappa}(u) + \frac{u_{i+\kappa+2} - u}{u_{i+\kappa+2} - u_{i+1}} B_{i+1,\kappa}(u)$$

This is carried on until B-splines of degree k are reached. The function ***splprep*** takes $k = 3$ by default and does not allow for $k > 5$ (see keyword k in Scipy-documentation n.d.).

3. Now, for every $u \in [0, 1]$, a corresponding point of an interpolated curve can be found as:

$$p(u) = (x(u), y(u)) = \left(\sum_{i=0}^{m} x_i B_{i,k}(u), \sum_{i=0}^{m} y_i B_{i,k}(u) \right)$$

Running this procedure (which can be done in a fairly straightforward manner since al the mathematics is performed automatically inside the ***splprep*** function) leads to positions of points on an interpolated curve, which can be plotted, such as on the Figure 5 right. To achieve this result, we are using a scatter plot with a sufficiently high frequency of sampling the B-splines between consecutive data points to achieve an illusion of a continuous line. (x, y) coordinates are converted to polar coordinates (r, θ) by setting $r = \sqrt{x^2 + y^2}$, and computing θ with the *NumPy* ***arctan2*** function.

It is important to make a notion that the *SciPy.interpolate* function ***splprep*** has an optional parameter s which defines a smoothing condition. By default, the curve will not be passing through all the points exactly, but will be adjusted to achieve a smoother curve. In our case, this is not a desired result. Instead we set $s = 0$, which forces the curve to pass through all the data points exactly, in accordance to the steps outlined above.

A careful reader might realize, that the plot on the left of Figure 5, obtained by connecting the consecutive VGP locations with straight segments, corresponds exactly to the use of B-splines but of degree 1, i. e. linear B-splines[1]. However, in our project when we talk about B-spline interpolation for the polar plot, we will always refer to the case of $k = 3$, i. e. a cubic B-spline. However, this observation is useful to mention for the sake of justifying our choice of B-spline interpolation. Essentially, a cubic B-spline is a smooth curve passing through each point. In general, a B-spline of degree k has continues derivatives up to the $(k-1)^{\text{th}}$ order. This is due to a nice property, that a derivative of a κ degree B-spline is a linear combination of B-splines of degree $\kappa - 1$ (which can be shown by mathematical induction) and the B-spline of degree 1 is continuous as it describes a segmented line passing from each point to the next one.

To summarize, we use cubic B-splines to interpolate the positions of the VGP to obtain a continuous curve with a continuous 2^{nd} derivative. This leads to a more elegant polar plot, as seen on the right of the Figure 5. An important caveat, however, is that this choice of interpolation leads to results (intermediate locations between established data points) which do not have a direct supporting evidence in the data. In principle, the intermediate locations are not physical, but mere results of different ways of interpolation, in both cases. This could only be avoided by drawing a scatter plot only, which however would fail to make a time series nature of the data presented intuitive. Nevertheless, an interpolation with straight lines does not subconsciously imply that the intermediate locations should be attributed with a physical meaning, whereas it could be inferred in such a misleading way from a plot obtained using cubic B-splines. Hence, in our code we leave an option to generate both kinds of plots, the choice being a trade-off between aesthetics and exactitude.

3.3 Animation

Besides static plots, we explored the possibility of presenting the evolution of the VGP location with animations. While generating animations in Jupyter Notebooks is somewhat awkward, and cannot be comprised in a class or even a function, we managed to create a piece of code which is optimized in a way that it does not require many modifications after copy-pasting to change a time period for which the animation is generated. We submit *.gif* files with the animations created for the entire time range of 49950 to 29950 years ago, and for several manually selected subperiods (before the Laschamp excursion (49950 to 41900 years ago), during (41900 to 40100 years ago) and after (40100 to 29950 years ago)), as accompanying files to this report, because a *pdf* is not a reliable environment for presenting dynamic animations. For illustrative purposes, however, we show exemplary frames of the animation for the entire time range in Figure 6. For animated gifs, the aesthetic advantage of cubic B-splines over straight lines is very apparent.

One important feature of the animations developed is that they show a path which has been traveled by the VGP over the entire time period covered by the data file, see green curves on Figure 6. Without that, the moving point or squiggle would be difficult to conceptually position in the broader context of the VGP location evolution. This feature has not only embellished the animations, but also inspired a feature of similar path curve visualisation in the widget application, which will be introduced in the next section.

[1] We also verified this observation by setting $k = 1$ for the ***splprep*** function, which reproduced the plot with straight lines

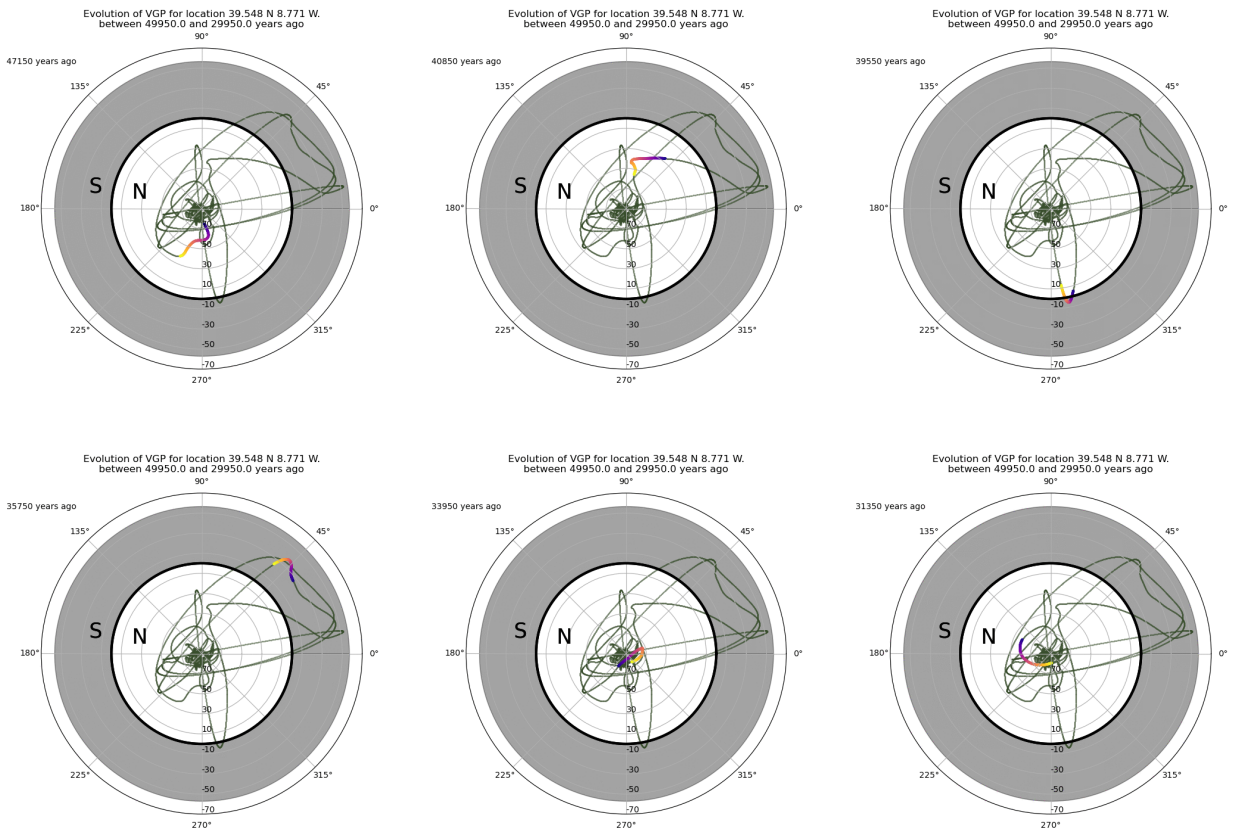

Figure 6: Example frames of the animation generated for the entire period covered by our data. The green curve corresponds to the (cubic B-spline interpolated) curve travelled by the VGP thorough that period. A colorful squiggle corresponds to the location at a moment in time mentioned on the left of each frame (yellow tip) and locations directly antecedent to that. Equator and areas corresponding to both hemispheres are indicated same as on Figure 5, see discussion in 3.2.1.

3.4 Visualizing VGP on the Earth's map in a widget application

Methods described in sections 3.2.1-3.3 plotted VGP location points only and lead to an outcome in a form of an image or *GIF*. As one final strategy to present this same result of a VGP calculation in a way which would have many advantages in terms of it's intuitiveness, we turned our attention towards presenting the VGP as a point on a 2D map of the Earth, this time aiming for a more interactive approach in the form of a widget application.

The resulting ***VGP Calculator Widget*** is a graphical user interface (GUI) application designed for the calculation and visualization of Virtual Geomagnetic Pole (VGP) coordinates. Developed using the Tkinter library for the GUI, with visualisation powered by Matplotlib with Cartopy, the application could provide a user-friendly platform for researchers and enthusiasts in the field of paleomagnetism.

As exemplified in Figures 7 and 8, the application layout consists of:

- The Earth map with contemporary continent layout in plate carrée projection (ArcGIS n.d.), where the site location is being displayed as a black dot, and, once calculated the VGP is displayed as a red dot.
- Two sliders for defining the site coordinates (site location and computed VGP values, if shown already, react immediately to the change of the slider). Initial values of those sliders correspond to the site in Portugal for which we had the data ($\lambda_{\text{site}} = 39°32.891'N$,$\varphi_{\text{site}} =° 46.266'W$).
- **Manual input** area. Here, a user can manually input inclination and declination values for a single sample so as to visualize where would a corresponding VGP fall, as on Figure 7:

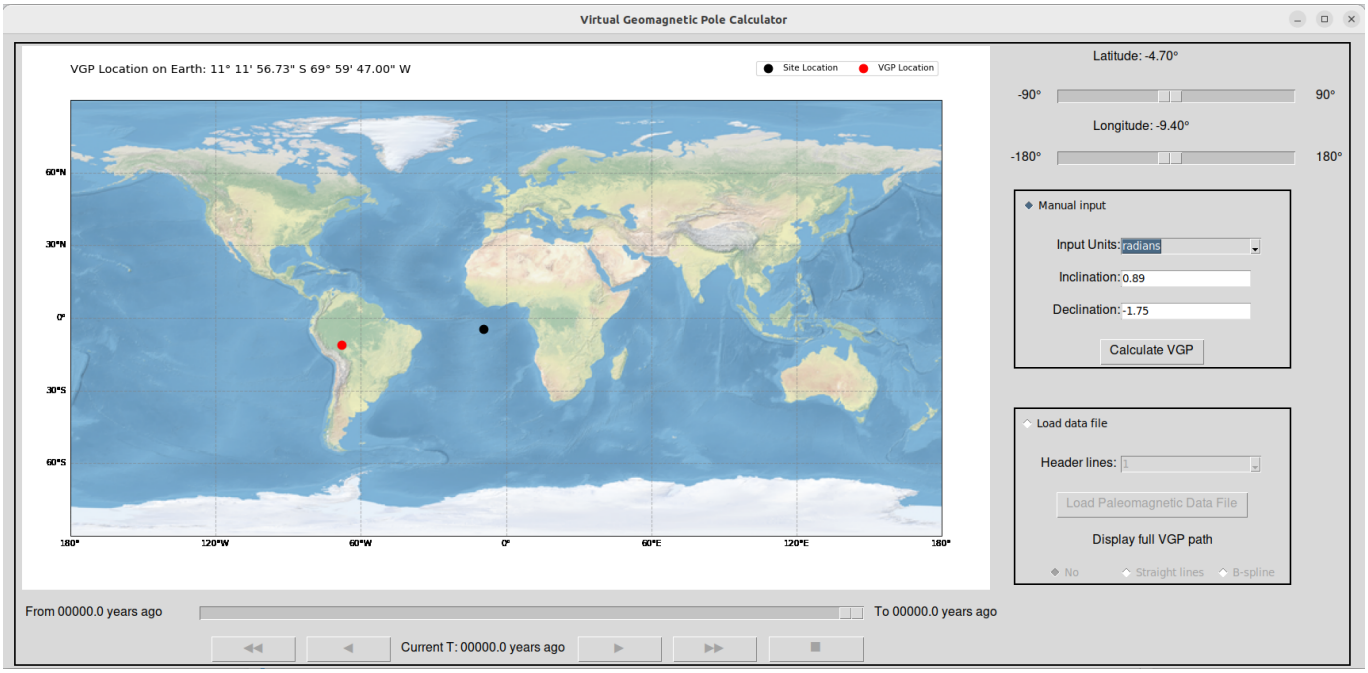

Figure 7: Application window in the manual input mode. Here, a hypothetical user favored providing inclination and declination in radians, adjusted the coordinate sliders to match a site at the Atlantic Ocean close to the equator, and generated a red dot corresponding to a calculated VGP. Parts of the application corresponding to the data file upload mode (widgets of the lower frame and the time slider) are disabled. Time labels are set to default values of 00000.0 until a file is loaded for the first time.

  - Radio button *Manual input* activates this section of the app and deactivates the other one (data file upload mode)
  - Dropdown menu *Input Units* allows to specify if the numerical values of the manual input should be interpreted as degrees (default) or radians
  - *Inclination* field - where the numerical value for inclination should be provided. When in the data file upload mode, the field is disabled, but an inclination value read from the data file for a given time T is displayed over it (see Figure 8)
  - *Declination* field - analogous
  - *Calculate VGP* button - each time new inclination and declination values are provided, this button must be pressed to update the VGP position shown on the map (and initially, before the first calculation, no red dot is present on the plot). However, if the position has already been calculated, and the user changes the unit in the *Input Units* dropdown menu, the VGP calculation and visualisation is updated immediately, without the need to press this button again

- Empty space between the **Manual input** and **Load data file** areas. If the user does not provide valid numeric strings in the inclination and declination fields, an error message *Wrong input, make sure all angles are valid numbers* will be displayed there. Not shown on Figures 7 and 8 as they exemplify proper use of the app without intentionally generating errors.

- **Load data file** area. Here, a user can upload a data file to be read by the application and used to generate a time series of VGP locations, as done by a hypothetical user on Figure 8:

  - Radio button *Load data file* activates this section of the app and deactivates the other one (manual input mode)
  - *Header lines* dropdown menu allows the user to specify a number $\in \{0, 1..., 5\}$ of header lines which should be skipped when reading the input file. Set to 1, which is the number of header lines in our *LSMOD2_predictions.dat* data file (and a reasonable guess for the number of header lines of any file), by default

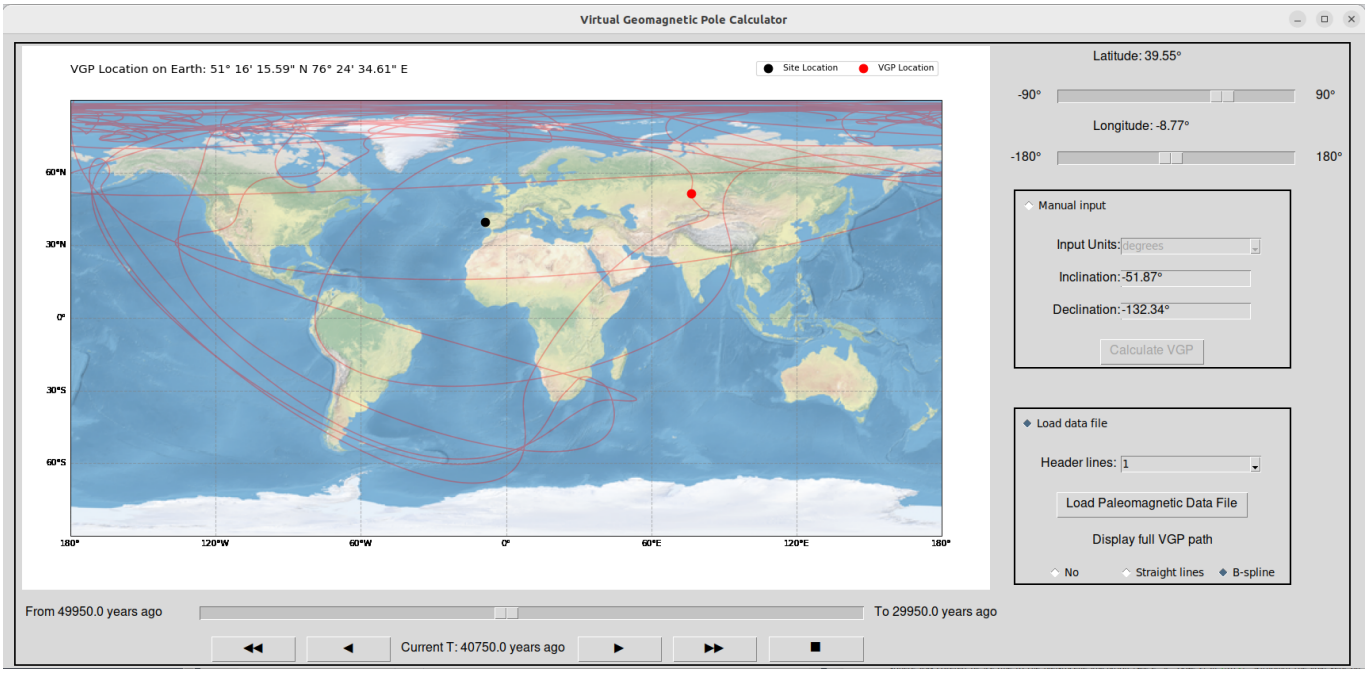

Figure 8: Application window in the data file upload mode. Here, a hypothetical user uploaded the file *LSMOD2_predictions.dat*, indicating that the file has 1 header line which needs to be skipped when processing the file, and leaving the coordinate sliders at their default values which correspond to the relevant site in Portugal. The VGP location corresponding to the end of the time interval got immediately calculated. He then chose to display the path of the VGP over the entire interval, with the B-spline interpolation choice which is analogous to cubic B-splines on the polar plots described in section 3.2.2. The user moved the time slider back to a point in time during the Laschamp excursion (see 4). Inclination and declination values corresponding to that moment in time, as read from the input file, are written over the corresponding disabled input fields of the manual input mode area.

  - *Load Paleomagnetic Data File* button, allowing a user to choose a file to be read. By default, only *.dat* files are sought after, facilitating selection of the *LSMOD2_predictions.dat* file
  - Set of radio buttons *Display full VGP path* is to allow for visualising the entire path travelled by the VGP during the time period covered by the data file, similarly as in the animation (see section 3.3, Figure 6):
    * *No* means no visualisation, default
    * *Straight lines* establishes visualisation with straight line interpolation between points, as on polar plots without the cubic B-spline, described in section 3.2.1
    * *B-spline* sets cubic B-spline interpolation analoguous as in 3.2.2, but within the plate carrée projection (ArcGIS n.d.) used in the application

- Empty space below **Load data file** area. If the data file chosen by the user is invalid (e. g. different file picked due to a misclick), or the information about the number of header lines provided is inaccurate[2], an error message *Your file seems to be invalid* will be shown there (again, not the case in Figure 7 or 8).

- Although positioned outside of the **Load data file** area (for the sake of accommodating more space for the slider), the widgets underneath the map also apply in the data file upload mode only. They relate to browsing the history of VGP evolution within the time period covered by the data file:

  - Dragging the slider lets manually select a chosen moment in time. Information about the time range for which the data is available is updated upon loading the file by changing the values of *From* and *To* labels (the information is taken from the input file directly, see 3.1. When the slider is moved, the label indicating the corresponding time (*Current T:*) is updated and so are the inclination and declination values displayed over the corresponding inactive input fields from the **Manual input** area

[2]Strictly speaking, if it is underestimated. If it is overestimated, the file should be processed just fine, merely the first line or two would then be skipped out (treated as part of the header) so the time period covered by the data loaded would be slightly shorter.

- Pressing the single arrow buttons allows for high precision movements of the slider, so as to move one time step (corresponding to data points available) at a time
- Pressing one of the double arrow buttons initiates an animation of the slider movement, where the slider keeps moving one step at a time (as if repeatedly pressing the corresponding single arrow button), until the end of the interval is reached, or the stop button (indicated with the square symbol) is pressed. As long as the animation is in progress, all other functionalities besides the stop button are disabled. Some patience is necessary when stopping the animation, because there is a bit of a delay before the app reacts to the pressing of the stop button. This slow way of animating would presumably be more useful for a careful inspection of the behaviour of VGP in a certain subperiod, rather than a quick visualisation of the entire interval, for which the animation introduced in 3.3 would be more suitable.

This summarizes the overview of the application and it's diverse functionalities. Before we proceed to the next section, we should mention that the choice of showing Earth's map as background in this last final approach evoked ambivalent thoughts. Initial reluctance sprung from a fact that the a layout of continents on the globe has not been constant in the past and will not be in the future, so presenting ancient data superimposed on a contemporary layout of our planet could be misleading. However, the continental drift due to plate tectonics is a process which takes time of the order of 10^7 years to lead to noticeable changes, and the configuration of Earth's landmass looked virtually the same 50000 years ago as it does now, aside of the fact that the major part of the northern hemisphere was covered by ice due to the pleistocene glaciation (see e. g. Böse *et al.* 2012).

Although the goal kept on the back of the mind when developing visualisation tools is that they should be applicable for any data, in most cases the time ranges corresponding to paleomagnetic data would be similar as in our study and the interpretation would therefore not change. In a rare case of trying to visualize magnetic pole positions over a much greater time period, one could still use the technique to which this section is devoted, but with a clear statement that the background map image is just for conceptual placement of the VGP on the globe, whereas the continent layout presented is no longer scientifically accurate. Alternatively, the tool could be modified by replacing the static image with an image drawn from a set of images, corresponding to a set of maps demonstrating the Earth's tectonic plate movement induced continental layout changes history, accordingly to the value of the time slider. Since we did not have data for which such a development would be imperatively needed, we carried on with using a single static image of a contemporary continental layout in the application.

4 Discussion of the results in the light of scientific knowledge

Our attempt to visualize the temporal evolution of VGP for the given location has revealed to us significant events in Earth's magnetic field history. Such events are known as geomagnetic excursions, being brief (1000s of years) deviations in geomagnetic field behaviour from what is expected during 'normal secular' variation. The Laschamp excursion ($\sim$ 41000 years ago) was a global deviation in geomagnetic field behaviour. This excursion adds complexity to our interpretation, influencing the VGP trajectory. Previously published records suggest rapid changes in field direction and a concurrent substantial decrease in field intensity. All models of Korte et al. 2019 suggest that the excursion process during the Laschamp is mainly governed by axial dipole decay and recovery, without a significant influence from the equatorial dipole or non-dipole fields. The axial dipole component reduces to almost zero, but does not reverse. This results in excursional field behavior seen globally, but non-uniformly at Earth's surface. Another significant event in the Earth's magnetic field history is the Mono Lake excursion, which may be a series of excursions occurring between 36000 and 30000 years ago, rather than a single excursion. In our case, we can identify a stark excursion around 34250 years ago. In contrast to the Laschamp, these excursions appear driven by smaller decreases in axial dipole field strength during a time when the axial dipole power at the core-mantle boundary (CMB) is similar to the power in the non-dipole field (Korte *et al.* 2019). Visualising the temporal evolution of VGP gave us the possibility to account all three phases suggested by Korte *et al.* 2019 for the period between 50 to 30 ka (kilo years, i. e. millenia) ago:

1. A broadly stable phase dominated by the axial dipole (50–43 ka) - the uppermost plot in Figure 9
2. The Laschamp excursion, with the underlying excursion process lasting $\sim$ 5 ka (43–38 ka) and the surface field expression lasting $\sim$ 2 ka (42–40 ka) - second plot from the top
3. For the third weak phase, during which axial dipole and non-dipole power at the CMB are comparable, the situation is somehow different. Instead of the number of excursions between 36 and 30 ka, we see only one sharp excursion (third plot on Figure 9). While the rest of the Mono Lake period (lowermost plot on Figure 9) shows

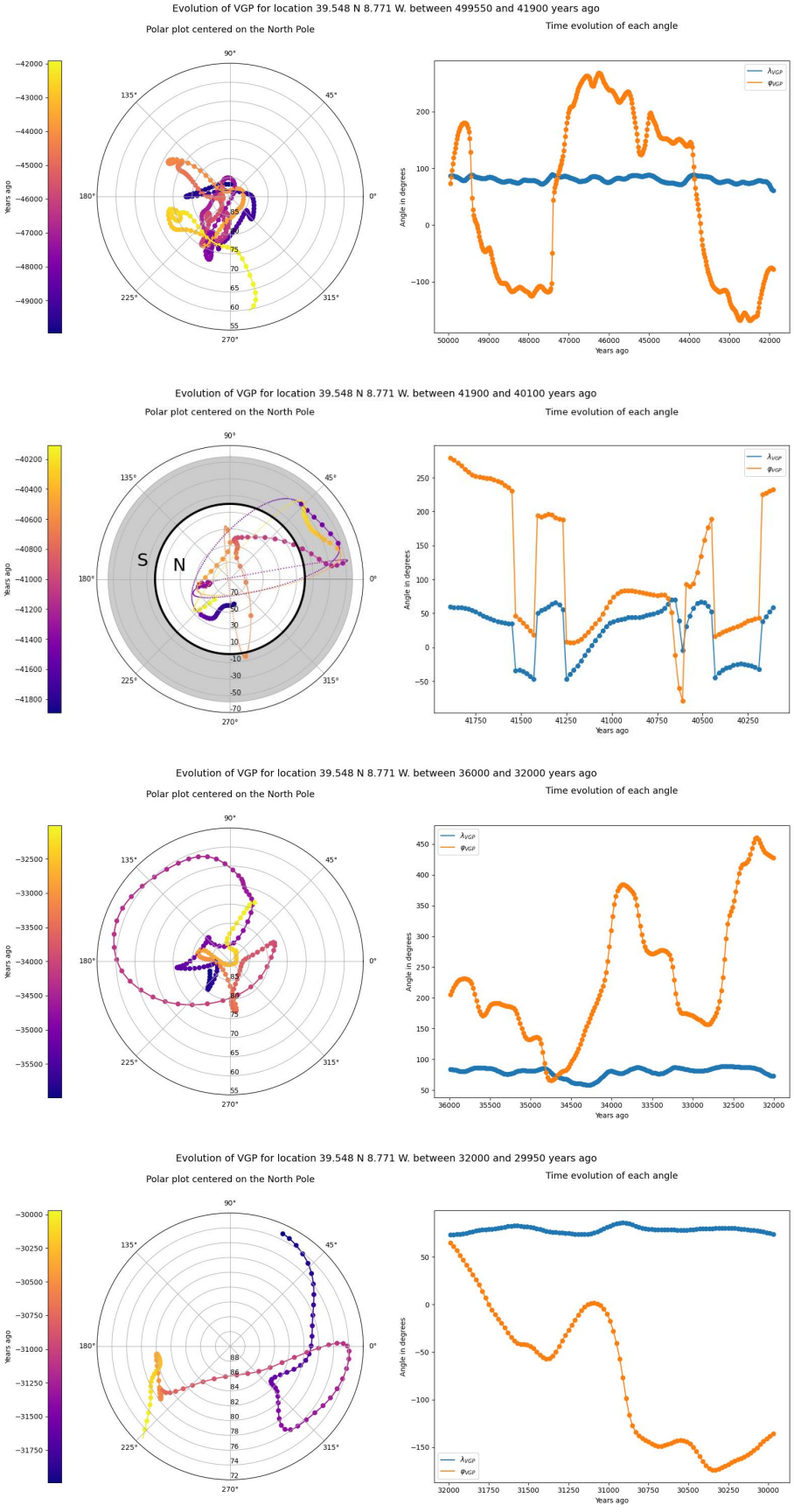

Figure 9: Visual representation of the VGP position variation at different characteristic periods as identified in Korte *et al.* 2019. The uniqueness of the appearance of the second plot is due to the fact that during the Laschamp excursion (see 4) the VGP transcended down to the southern hemisphere, see discussion in 3.2.1. We're skipping the period between 40100 and 35000 to comprise all periods of interest on one page.

some long term variations, there are no extreme excursions visible during that time based on the data for a single location which we had at our disposal. However, accurate dating of excursions and determinations of their durations from multiple locations is necessary for a good understanding of the global field behaviour during these deviations.

A joint plot covering an entire time range (49950 to 29950 years ago), with all of those periods, is presented on the Figure 10

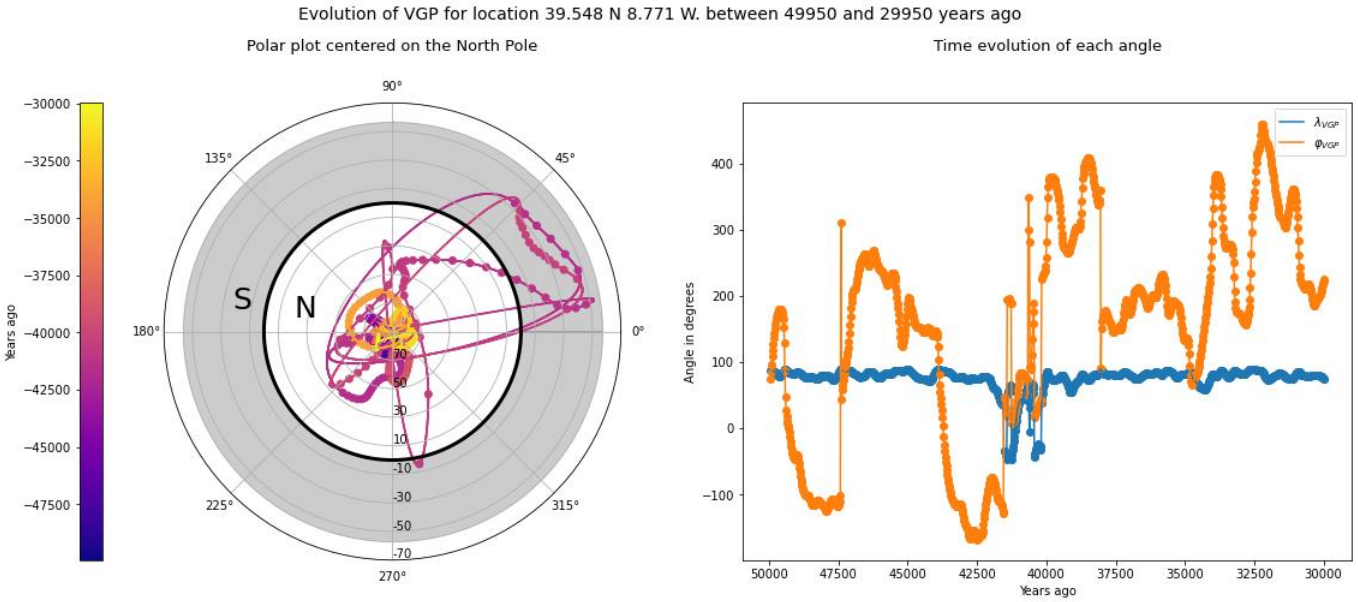

Figure 10: Similar plot as those on Figure 9, but covering the entire time range of our data, including the Laschamp (42-40 ka) and Mono Lake (34 ka) excursions. The continuity of the φ_{VGP} is handled here a bit differently (compare the feature on the simple plots here and on the third plot on Figure 9 around 34250 years ago), but the alternative would lead to an unnecessarily big vertical scale, with angles reaching close to 720°.

5 Conclusions and perspectives for future development

Our investigation into the time evolution of the virtual geomagnetic pole (VGP) in Portugal, between 50 to 30 millenia ago, provides insights into the complex nature of Earth's magnetic field.

- **Geomagnetic Models and Interpretation:**

  Examining different models, such as the geocentric axial dipole, inclined geocentric dipole, and eccentric dipole, has highlighted the importance of considering the non-dipole field. While the eccentric dipole enhances alignment with measurements, the remaining non-dipole field underscores the inherent complexity of Earth's magnetic behavior.

- **Site-Specific Considerations:**

  Modeling the inclined geomagnetic dipole and geomagnetic pole involves averaging measurements from different locations, introducing the concept of virtual geomagnetic poles (VGPs). Our study, based on data from Portugal, underscores the challenge of inferring a global model from a single site, highlighting the site-specific nature of paleomagnetic data.

- **Interpretation of Portugal's Paleomagnetic Data:**

  The calculated VGPs offer valuable insights into the magnetic field's evolution in Portugal during the specified period. The visualizations provide a dynamic representation of how the geomagnetic pole's position changed over time, contributing to our understanding of regional magnetic variations.

Moving forward, our project opens avenues for future development:

- **Enhancing Code Robustness:**

  The Python program developed for VGP visualization can be further refined to provide a more robust framework for computing and visualizing both virtual and actual geomagnetic poles' temporal evolution. One desirable improvement would be increasing the flexibility on the type of input file accepted by the code - currently only files organized in the same way as *LSMOD2_ predictions.dat* are going to be parsed properly, but there are other conventions within the paleomagnetic community which should be accounted for, that would require additional intermediate calculation and data processing steps to reach analoguous results.

- **Expanding Dataset and Geographic Coverage:**

  To achieve a more comprehensive understanding of Earth's magnetic field dynamics, datasets from various locations and time periods should be used. This would contribute to a more accurate representation of global geomagnetic processes and give us the possiblity to track some important events of Earth's magnetic field evolution.

- **Integration with Advanced Models:**

  Incorporating advanced geomagnetic models and methodologies into the code can enhance accuracy and broaden the applicability of our visualizations. Collaboration with experts in paleomagnetism and geophysics could facilitate the integration of state-of-the-art modeling techniques.

In conclusion, our findings provide valuable insights into the paleomagnetic history of Portugal, emphasizing the need for nuanced models and acknowledging the challenges of site-specific data. Future developments should aim at refining and expanding our approach to contribute to a deeper understanding of Earth's magnetic field dynamics. The Earth's magnetic field is crucial for the habitability of our planet, as it acts like a shield protecting us from the charged particles coming from the sun. During the Laschamp excursion strength of the Earth's magnetic field almost vanished, which led to a big increase in cosmic and solar particles bombarding our planet. If such an event happens again during our lifetime, it will have significant consequences. For that reason, it is highly important to study the history of Earth's magnetic field and understand its mechanisms.

References

ArcGIS (n.d.). `https://pro.arcgis.com/en/pro-app/3.1/help/mapping/properties/plate-carree.htm`Plate carrée projection.

Böse, Margot *et al.* (June 2012). "Quaternary glaciations of northern Europe". In: *Quaternary Science Reviews* 44, pp. 1–25. DOI: `10.1016/j.quascirev.2012.04.017`.

Butler, Robert F. (1992). *PALEOMAGNETISM: Magnetic Domains to Geologic Terranes*. Blackwell Scientific Publications.

Korte, Monika *et al.* (2019). "Robust Characteristics of the Laschamp and Mono Lake Geomagnetic Excursions: Results From Global Field Models". In: *Frontiers in Earth Science*. Specialty section: Geomagnetism and Paleomagnetism, article number. DOI: `10.3389/feart.2019.00110`.

Maths, Plus (n.d.). `https://plus.maths.org/content/maths-minute-map-projections`Map projections.

Scipy-documentation (n.d.). `https://docs.scipy.org/doc/scipy/reference/generated/scipy.interpolate.splprep.html`*splprep* function for preparing a B-spline representation of a curve.